Terr. Atmos. Ocean. Sci., Vol. 23, No. 3, 291-301, June 2012 doi: 10.3319/TAO.2011.11.02.01(A)

Toward a Multi-Decadal Climatology of North Pacific Polar Lows Employing Dynamical Downscaling

Fei Chen[1, *], Beate Geyer[1], Matthias Zahn[2], and Hans von Storch[1]

[1] *Institute of Coastal Research, Helmholtz-Zentrum Geesthacht, Germany*
[2] *University of Reading, Harry Pitt Building, Reading, UK*

Received 29 July 2011, accepted 2 November 2011

ABSTRACT

The North Pacific is an area where sub-synoptic Polar Lows frequently form during the cold season, especially over the Bering Sea, Gulf of Alaska and Japan Sea. So far, a multi-decadal climatology of such Polar Lows based on individual cases has not been assembled. Here, we consider dynamical downscaling method for realistically constructing the formation and life cycles of such lows over the past 6 decades without exploiting sub-synoptic information in initial fields. To do so, a regional climate model is conditioned by large-scale information of NCEP re-analyses. We test the approach by examining its skill in simulating ten known cases of North Pacific Polar Lows. Three of these are discussed in some detail.

The signatures of all storms emerge in the simulations with additional sub-synoptic details. The tracks of the simulated Polar Lows closely follow the tracks derived from satellite imagery. We conclude that the suggested method is suitable for constructing multi-decade climatologies, including trends and variability, of Polar Lows in the North Pacific by dynamically downscaling NCEP re-analyses.

Key words: North Pacific, Polar Low, Downscaling, Tracking algorithm, Regional climate modeling

Citation: Chen, F., B. Geyer, M. Zahn, and H. von Storch, 2012: Toward a multi-decadal climatology of North Pacific Polar Lows employing dynamical downscaling. Terr. Atmos. Ocean. Sci., 23, 291-301, doi: 10.3319/TAO.2011.11.02.01(A)

1. INTRODUCTION

1.1 Purpose of This Study

Polar Lows are intense sub-synoptic-scale cyclones, which occur over sub-polar oceans during the cold season. They form in cold air masses pole-ward of the polar front. These cyclones go along with strong winds. Therefore they constitute a significant risk for shipping and offshore activities.

Since the advent of satellites, Polar Lows can be identified relatively easily, and short-term risk management can be performed. However, risk assessment is problematic since a homogeneous description of the formation and spatial distribution of such disturbances has not yet been achieved. Even if one could screen all satellite imagery, one would be left with very incomplete weather maps prior to the advent of satellite use. Indeed, North Pacific Polar Low studies have been limited to either specific cases or to statistics covering only a few years (1976 - 1983; Yarnal and Henderson 1989a; Fu et al. 2004b).

Polar Lows in the North Atlantic (Zahn and von Storch 2008b) as well as for typhoons in East Asia (Feser and von Storch 2008) are two such sub-synoptic phenomena, thus a methodology has been developed recently to construct a homogeneous data base for the formation and life cycles of such sub-synoptic disturbances. "Homogeneous" refers here to the property that changes in the data base are most likely reflecting changes in the physical reality and not changes in the observational-analytical process. Thus a homogeneous data base would have the same error statistics in 1960 as in 2000, and no improvement would be implemented in the course of the analysis; the reason is, of course, that we want to attribute changes in the data base to changes in the physical system and not to unknown technical and procedural causes like changing density of observations or ever improving quality of instruments.

* *Corresponding author*
E-mail: Fei.Chen@hzg.de

We have launched an effort aimed at creating such a multi-decadal climatology for the North Pacific, and use the dynamical downscaling method developed and tested by Zahn et al. (2008) for the North Atlantic. This method is based on the observation that a standard multi-year re-analysis, such as NCEP with a grid resolution of T62 (about 1.875°), is insufficiently describing sub-synoptic-scale phenomena like Polar Lows, but provide a homogeneous description of the large-scale flow conditions. The method consists of running a regional climate model (RCM) over the North Pacific Ocean, and dynamically downscale the NCEP 1 re-analysis data (Kalnay et al. 1996).

The analysis is done in two steps, following the example of Zahn et al. (2008). First a series of polar low cases is considered and whether the downscaling procedure captures the details of the formation and lifecycle of the polar lows well. When this hurdle is surmounted, the simulation is extended to cover all six decades of NCEP-re-analyses enabling the study of changing statistics of the North Pacific polar lows.

In the present paper we report about step 1 and demonstrate that the Zahn et al. (2008) method performs well also in the North Pacific. We have simulated cases of life cycles of Polar Lows, and their movement across the ocean. The model is initiated well in advance of the formation of the cyclones, so that the generation of the lows is not due to some seeds in the initial field, but dynamically induced by favorable large-scale conditions [which are enforced on the regional model by "large-scale nudging" (von Storch et al. 2000) towards the driving NCEP re-analysis]. It turns out that the Polar Lows are realistically described by the regional model, with considerably more detail than in the driving NCEP re-analysis. We conclude that launching a multi-decadal simulation for studying the variability of annual statistics of Polar Lows in the Northern North Pacific is warranted as a second step which has been initiated with a paper forthcoming at a later date.

Sometimes our study is misunderstood in that we would appear to add more cases to the existing list of case studies on Polar Lows. This is not the case, the purpose is also not to describe detailed dynamical properties and life cycles, or to discuss and test different dynamical mechanisms responsible for the formation; instead the purpose is to demonstrate the potential to construct a climatology in order to derive trends of Polar Low statistics in the past decades, as well as the possibility to derive consistent scenarios for the present century. In a subsequent publication, we will present a climatological model, including trends and low frequency variability of Polar Lows in the North Pacific from 1948 to 2011.

In section 2, the experimental approach (model and cases) is briefly sketched. The simulations of three cases from 1975, 1977 and 1997 are discussed in section 3, and the results of all ten cases are discussed in section 4.

1.2 Present Knowledge: Mechanisms, Regions and Case Studies

During past 5 decades, several theories have been used to explain Polar Low development, such as: baroclinic instability, barotropic instability, Conditional Instability of the Second Kind (CISK) or Wind Induced Surface Heat Exchange (WISHE) instability (Forbes and Lottes 1985; Bond and Shapiro 1991; Kolstad 2006; Kolstad et al. 2009; Wu and Petty 2010). Various case studies indicate that usually several mechanisms together lead to the formation of Polar Lows (Nordeng 1990; Mailhot et al. 1996). Polar Lows have a relatively short life cycle (usually less than 2 days) and spatial scales of 200 - 1000 km, which is smaller than the scales of the baroclinic "polar front" lows.

So far, a great part of observed knowledge about Polar Lows is based on the analysis of satellite imagery. Polar Lows over the Northern North Pacific Ocean are characterized by a tight, spiral or comma cloud pattern; comma cloud features are predominate in the Bering Sea and Gulf of Alaska and both the spiral and comma pattern are found in the Japan Sea (Businger and Walter 1988; Douglas et al. 1991). Satellite-based climatologies have been derived for relatively short periods of time (Carleton 1985; Yarnal and Henderson 1989b). Most active Polar Low cyclogenesis takes place in the western mid-latitude North Pacific, with a maximum of Polar Low cyclogenesis located just off the east coast of Japan's northernmost island Hokkaido. The eastern North Pacific is less active with Polar Lows forming infrequently in the Gulf of Alaska. Since Polar Lows usually form in cold air masses moving from cold continents or ice-covered regions over open water, this pattern of formation reflects mostly the geographically different sea surface temperature conditions.

In a number of case studies it was demonstrated that Polar Lows can be described by dynamical high-resolution models [for the Japan Sea, see Fu et al. (2004a), Yanase et al. (2004), Yanase and Niino (2007); the Bering Sea see Bresch et al. (1997); the Gulf of Alaska see Businger (1987) and Blier (1996)]. In all cases the model results were consistent with satellite observations. Different from our approach, these studies make use of initial conditions describing the specific synoptic situation, within which the Polar Low forms, or first traces of the Polar Low itself. Consequently, unlike our study, these models are initiated right before the actual Polar Lows began to develop.

2. THE EXPERIMENTAL SETUP: USED MODEL, TRACKING AND CASES

2.1 Model Used

In this study we used the COSMO-CLM model (Steppeler et al. 2003; Rockel et al. 2008). The COSMO-CLM (COSMO model in CLimate Mode) is the climate version

of the operational weather prediction model of the German National Weather Services and the COnsortium for SMall scale MOdelling (COSMO), adapted to climate simulation purposes by the CLM-Community (www.clm-community.eu). The model equations are formulated in rotated geographical coordinates and a generalized terrain following height coordinate. Its prognostic, non-hydrostatic equations feature the variables horizontal and vertical Cartesian wind components, temperature, pressure perturbation, specific humidity, cloud ice content and specific cloud liquid water. Initial and lateral boundary conditions are given by the NCEP 1 re-analysis data.

COSMO-CLM has been widely used for climatic studies not only over the European continent, Mediterranean Sea and Atlantic Coast (Rockel et al. 2008), but also for studying North Atlantic Polar Lows (Zahn and von Storch 2008b), East Asian typhoons (Feser and von Storch 2008) and "Medicanes" in the Mediterranean Sea (Cavicchia and von Storch 2012).

The simulation region is shown in Fig. 1. A rotated grid with 0.4° grid resolution and a longitudinal and latitudinal grid of 220 and 80 points are employed. The region includes the Bering Strait in the north, the winter low pressure system "Aleutian Low" with its great influence on the formation of Polar Lows, and the Japan Sea.

The time step is 100 s for integration, and the output time interval is 1 hour. All the initial and boundary conditions were provided by the NCEP 1 re-analysis data. The large-scale constraining technique named spectral nudging (von Storch et al. 2000) has been used in order to keep the large scale variability close to the NCEP re-analysis, which is available four times a day, and is interpolated to the shorter model time step. The spectral nudging is applied at 750 hPa and above, with the nudging becomes stronger with height. It is limited to horizontal wind velocities and spatial scales larger than 800 km.

All simulations were begun several weeks before the formation of the Polar Low, so the formation of the Polar Low has is not a result of specific configuration of the initial state. Weisse and Feser (2003) have shown that ensemble variability becomes negligible, when the RCM is employing spectral nudging [see also Feser and von Storch (2008); Zahn et al. (2008)].

2.2 Tracking Polar Lows

It is not very challenging to find the Polar Lows in the satellite images - we knew the location and time. However, it is much more difficult to detect them from complex and large output of the model simulation. We test if the detection and tracking-algorithm previously developed by Zahn and von Storch (2008a), for finding Polar Lows in the output of COSMO-CLM simulations automatically also works for our cases. The tracking algorithm works in three steps:

First the local minima are identified in the band-pass filtered mean sea level pressure field. This selective scale analysis is done to identify the sub-synoptic polar lows and differentiate them from regular synoptic storms. A digital band pass filter (Feser and von Storch 2005; Feser 2006) was used; the wave-numbers we used for the filter is between 6 and 15, which retained variability of spatial scales from 300 to 700 km. In the second step the detected positions of pressure minima are combined time-step by time-step to form tracks. We applied hourly time step here instead of the default 3 hour which Zahn used.

In the third and final step, some constraints are employed to remove remaining synoptic cyclones. Tracks whose filtered minima pressure do not fall below a threshold

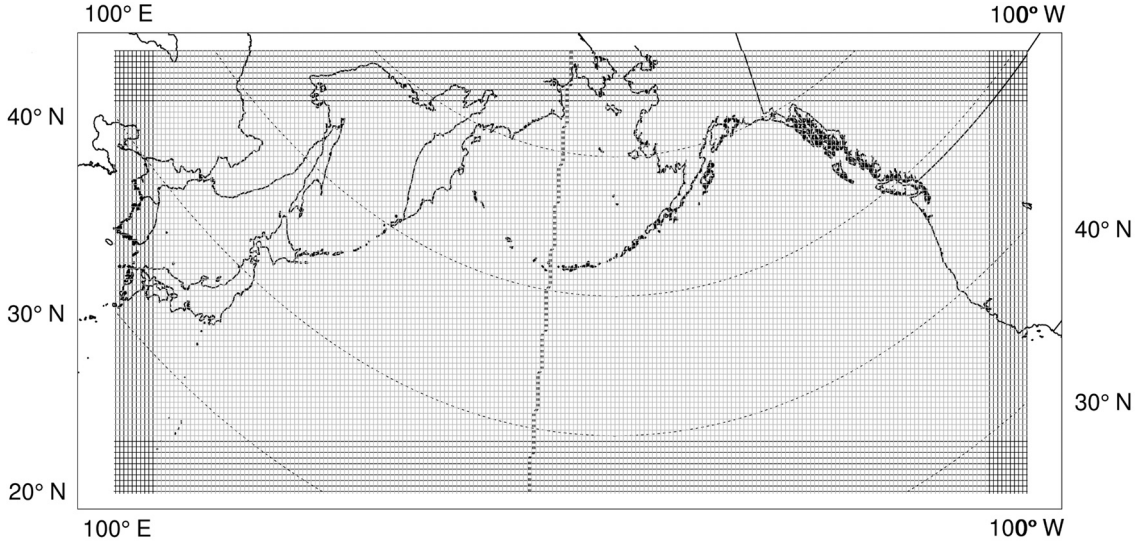

Fig. 1. Simulation area and model grid used for this study. Darker grid boxes at the border represent the sponge zone.

value of -2 hPa at least once have been excluded. Second, a 10-meter-high wind speed must exceed the gale force standard at least 20% along the tracks. Thirdly for the difference between the sea surface temperature (SST) and 500 hPa temperature we choose a somewhat weaker threshold compared to Zahn and von Storch (2008a) of 39 K, which must be exceeded at least once. If the filtered minimum is very low, less than -6 hPa, all other constraints listed above are overridden. Finally, based on the definition of Polar Low, the tracks must follow a north-south direction and strike no land along the track.

3. RESULTS

Ten different cases of North Pacific Polar Lows were simulated to check the reliability of our simulations. They are listed in Table 1. Of these, three cases have been selected (marked by an asterisk in the Table) to be discussed in more detail below. Most of these cases can be clearly reproduced and tracked.

Three cases of the ten Polar Low formation in the North Pacific, in March 1975, March 1977 and January 1997 are presented here. They were selected from the regions with highest frequency of Polar Low formation: the Gulf of Alaska, Bering Sea and Japan Sea. The performance of the model in these three cases may be taken as indication of the model's capability of describing such sub-synoptic-scale phenomena realistically.

We compare our simulations with both the original NCEP 1 re-analysis data as well as with detailed analyses in the literature.

3.1 Case 1: 6th - 7th March 1977

The first case is a Polar Low on 6 - 7 March 1977 in the Bering Sea, which was examined by Bresch et al. (1997). Our simulation was initialized on 1st February 1977, more than 1 month before the formation of the Polar Low.

Figure 2 shows the relatively coarse-grid NCEP 1 reanalysis air pressure field on 0600 UTC 7th March. A large

Table 1. Examined cases of Polar Low formation. The asterisk (*) marks the 3 cases, which are discussed in detail in this paper. The characters O, N and S represent the data taken either from the detailed analysis in the references (O = observation), from the NCEP-1 reanalysis (N) and from the downscaling simulation (S).

	Date	Region	Location of cyclogenesis	Max wind speed (m s^{-1})	Central pressure (hPa)	Reference
1*	22 March 1975	Gulf of Alaska	(154°W 54°N) Same position as in observation	O: 25 N: 21 S: 22	O: 980 N: 1005 S: 995	Businger (1987)
2*	7 March 1977	Bering Sea	(165°E 50°N)	O: ---- N: 12 S: 14	O: ---- N: 1006 S: 998	Bresch (1997)
3	23 January 1979	Bering Sea	(174°E 56°N) Same position as in observation	O: ---- N: 15 S: 16	O: ---- N: 997 S: 997	Businger (1987)
4	12 March 1985	Gulf of Alaska	(165°W 54°N) 3° north compared to the observation	O: 25 N: 40 S: 20.7	O: 995 N: 1007 S: 993.8	Steven and Bernard (1988)
5	4 March 1987	Gulf of Alaska	(140°W 54°N) Same position as in observation	O: ---- N: 21 S: 13	O: --- N: 1003 S: 1001	Douglas et al. (1991)
6	1 December 1987	Gulf of Alaska	(141°W 49°N) Same position as in observation	O: 36 N: 9 S: 26	O: 959 N: 961 S: 958	Bond and Shapiro (1991)
7	27 February 1996	Japan Sea	(128°W 39°N) Same position as in observation	O: ---- N: 7.6 S: 9	O: ---- N: 1014 S: 1016	Fu et al. (1999)
8*	21 January 1997	Japan Sea	(139°E 42°N) Same position as in observation	O: 12 N: 8 S: 9	O: 998 N: 1006 S: 1008	Fu et al. (2004a)
9	10 February 1997	Japan Sea	(138°E 40°N) 3° west compared to the observation	O: ---- N: 20 S: 12	O: ---- N: 1008 S: 1010	Fu et al. (2004b)
10	19 December 2003	Japan Sea	(139°E 38°N) 2° southwest compared to the observation	O:20 N:12 S:16	O: 996 N: 1007 S: 1003	Guo et al. (2007)

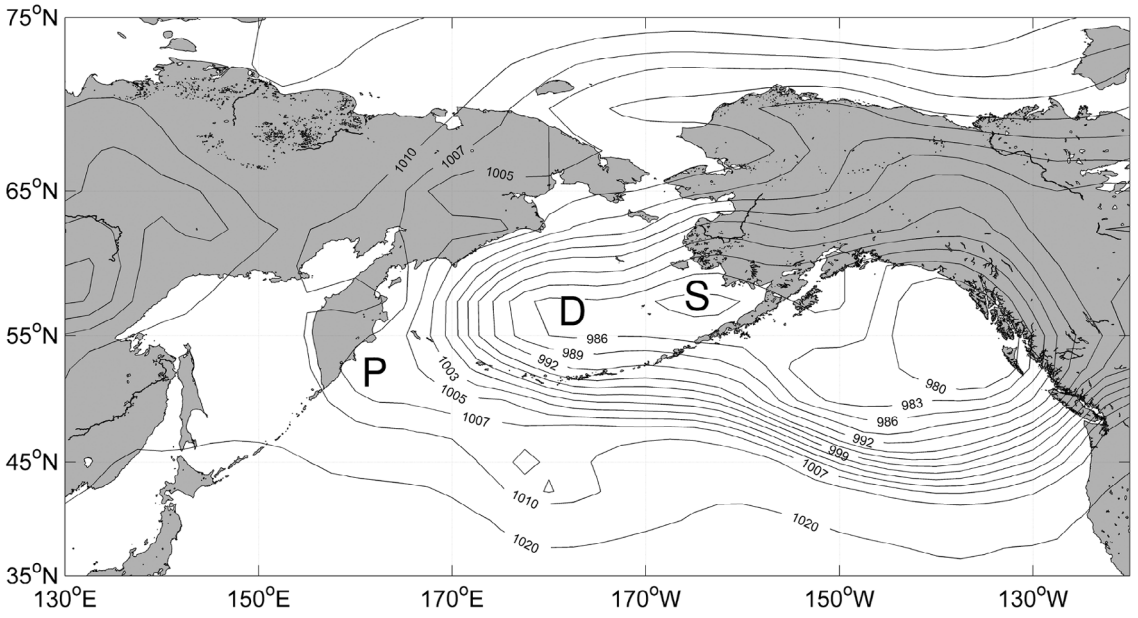

Fig. 2. Mean sea level pressure (SLP) as described by NCEP 1 re-analysis with a 1.875° grid resolution on 0600 UTC 7th March 1977, when a Polar Low formed west of the Kamchatka Peninsula. P represents the Polar Low, S represents the synoptic low and D represents a Polar Low discussed by Bresch et al. (1997).

synoptic low is located in the Bering Sea (see "S" in Fig. 2). The location of the Bering Sea low S is stable over the next 36 hours. In the southward air stream at its western flank, there are two diffuse depressions D and P located to the east and southeast of the Kamchatka Peninsula. A tracking of both D and P in NCEP analysis is hardly possible. The general pattern of Fig. 2 is substantiated by a satellite image provided by Bresch et al. (1997) - see Fig. 3, where both D and P are marked, but it becomes obvious that the features described by NCEP are much too diffuse.

The downscaling simulation with the limited area model provides more sub-synoptic-scale detail (Fig. 4). We find the same synoptic situation as in Bresch et al. (1997), with the large scale low in the Bering Sea moving cold air southward at its western flank.

The 0600 UTC 6th March simulated sea level pressure field (Fig. 4) shows a mature state synoptic low S, and a sub-synoptic-scale pressure minimum P, at approximately around (156°E, 50°N). Later the simulated Polar Low P was moving southeast-ward and becoming weaker. The 1200 UTC model results show a weaker but still a spiral structure Polar Low. After 1800 UTC, the low travelled over the sea and moved east-ward along the 50°N latitude line. At 1000 UTC 7th March, the position is around 172°E, 50°N, generally the same as the satellite image at 0958 UTC (Fig. 3). This track is well detected by the automated detection and tracking algorithm (not shown).

The sub-synoptic-scale swirl D, as shown in Fig. 3, is reproduced by our simulation only to a very limited extent, namely as a very weak disturbance of the isobars at 1000 UTC on 7th March 1977 (Fig. 4). Interestingly, Bresch et al (1997) focused on the D-case, and addressed "our" P case only in passing.

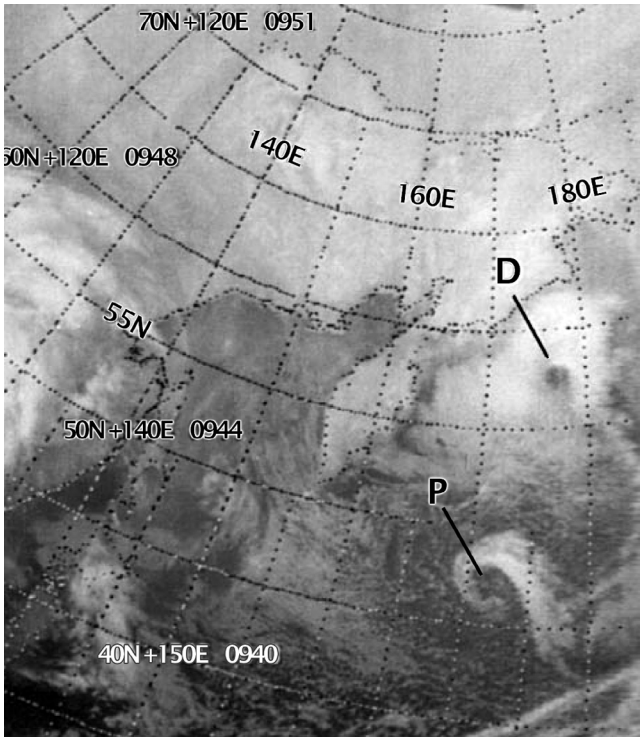

Fig. 3. NOAA-5 infrared satellite image at 0958 UTC 7th March 1977; "D" marks the Polar Low in Bresch et al. (1997) and "P" the cloud pattern of the Polar Low we get (taken from Bresch et al. 1997).

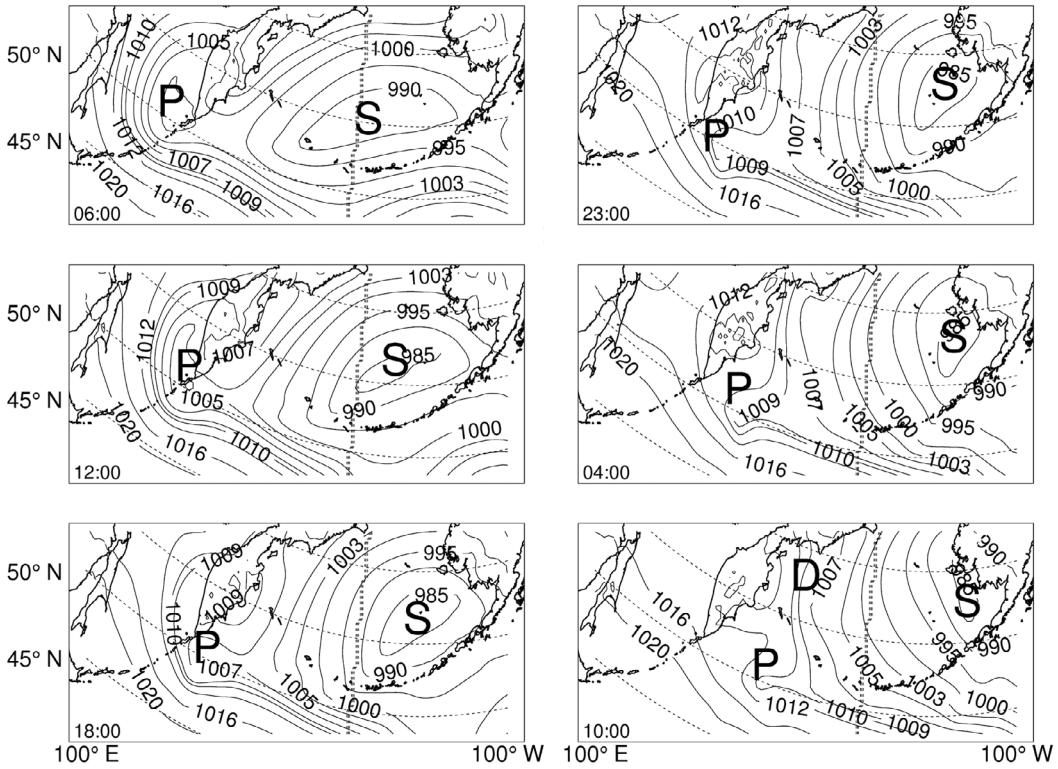

Fig. 4. Mean sea level pressure (SLP) of COSMO-CLM simulation results from 0600 UTC 6th to 1000 UTC 7th March 1977, P represents the Polar Low, S represents the synoptic low and D represents the Polar Low in Bresch et al. (1997). Left column: maps for 0600, 1200 and 1800 UTC on 6th March 1977; right column: 2300 UTC in 6th March, 0400 and 1000 UTC on 7th March 1977. The satellite image in Fig. 3 corresponds to the phase between the middle and bottom map on the left.

3.2 Case 2: 22th March 1975

In this section, we will discuss the case of a Polar Low which formed on 22th March 1975 south of Alaska (Businger 1987). The satellite images (Fig. 5) shows the mature stage of this Polar Low, labeled as "P." It lasted nearly 48 hours.

The COSMO-CLM results (Fig. 6) showed the initial, mature and decay stages of the Polar Low "P." The centre pressure minimum is below 995 hPa and the spatial scale is about 500 km. It is hardly detectable in the NCEP 1 re-analysis air pressure field (not shown), but well reproduced by our regional model and tracked by the algorithm.

Polar Lows usually take place during cold air outbreaks, with a movement southward from ice covered land to the open ocean. Quite uncommonly, the track of this Polar Low has a slight northward component. This situation may be due to the steering synoptic circulation system "S."

From the simulation result we found that it was induced by a 500 hPa upper level cold core vortex (not shown). The track is southward across the Japan Sea and ends on Japan Island. Likely reflecting the narrow Japan Sea, the Polar Low decayed quickly after having reached Japan Island.

Compared to Fu et al. (2004a), this Polar Low also had a weak signature at the surface in the Regional objective analysis (RANAL) data of JMA (Japan Meteorological Agency). When compared to the simulation result by Yanase et al. (2004), we found this Polar Low is visible in the 5 km resolution grid.

In the COSMO-CLM a weak disturbance shows up at the observed position of the low (Fig. 8). This signature is too weak to be tracked by our automated algorithm. However, it is clearly visible - as a cold core vortex at the 500 hPa upper level (Fig. 9). The simulated track shows the Polar Low moving realistically southward across the Japan Sea.

3.3 Case 8: 21th January 1997

The third case took place on 21 January 1997, when a Polar Low moved across the Japan Sea (Fu et al. 2004a). Figure 7 shows in a satellite imagery sequence the mature stage of this Polar Low. The Polar Low on 21 January 1997 lasted less than 32 hours.

4. DISCUSSION

As a preparative analysis for the feasibility of simulating and investigating long term trends and variability of Polar Lows in the North Pacific, we have examined the performance of a dynamical downscaling system, which makes use of the NCEP 1 re-analysis data as forcing of the COS-

MO-CLM limited area model. The objective is to generate sub-synoptic scale descriptions of Polar Lows, without making use of high-resolution initial fields. In three case studies of Polar Low formation and life cycle, we found that due to the higher spatial resolution considerably more detailed in the simulation compared to the re-analysis description. Also the hourly output turns out to be helpful compared to the routine 6 hourly output from NCEP reanalysis.

We examined three cases in some detail; seven others were similarly examined but for reason of brevity not discussed in this paper. Nevertheless, results for all 10 cases are summarized in Table 1. In six cases, the Polar Lows are well reproduced, and their tracks of the Polar Low were detected in the downscaling COSMO-CLM result with our automated detection and tracking tool. The tracks were very similar to the satellite observations. The four other relatively weak cases are also simulated, but the signatures are too weak to become reliably detected with our tracking method. In particular the CCLM simulation of case 8 had a very weak signature at the surface at the surface, and but a signature clearly emerging at higher levels, such as 500 hPa and consistent with the detailed analysis by Fu et al. (2004a).

The downscaled polar lows showed in 7 out of 10 cases a stronger wind than in the NCEP-reanalysis and were thus closer to the configurations described in the literature, and

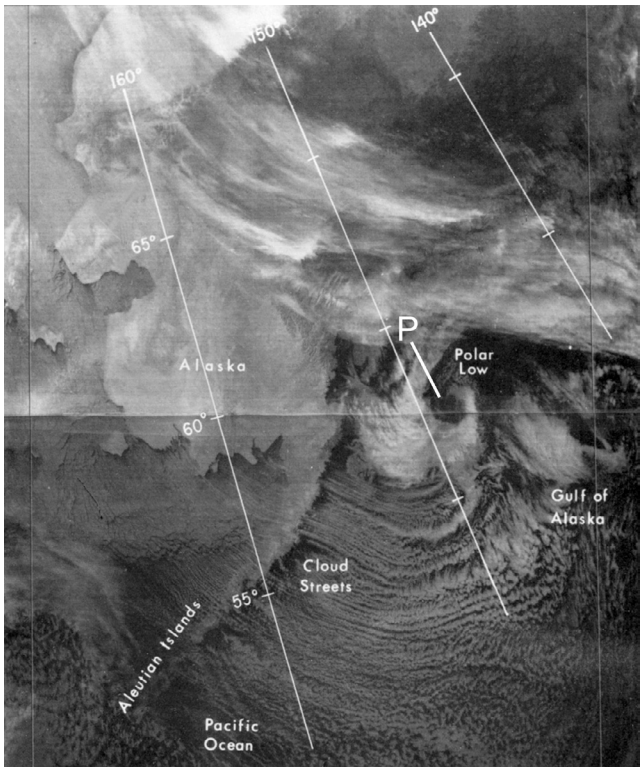

Fig. 5. NOAA-4 infrared satellite image at 20.21 GMT on 6th March 1975, P represents the Polar Low (Businger 1987).

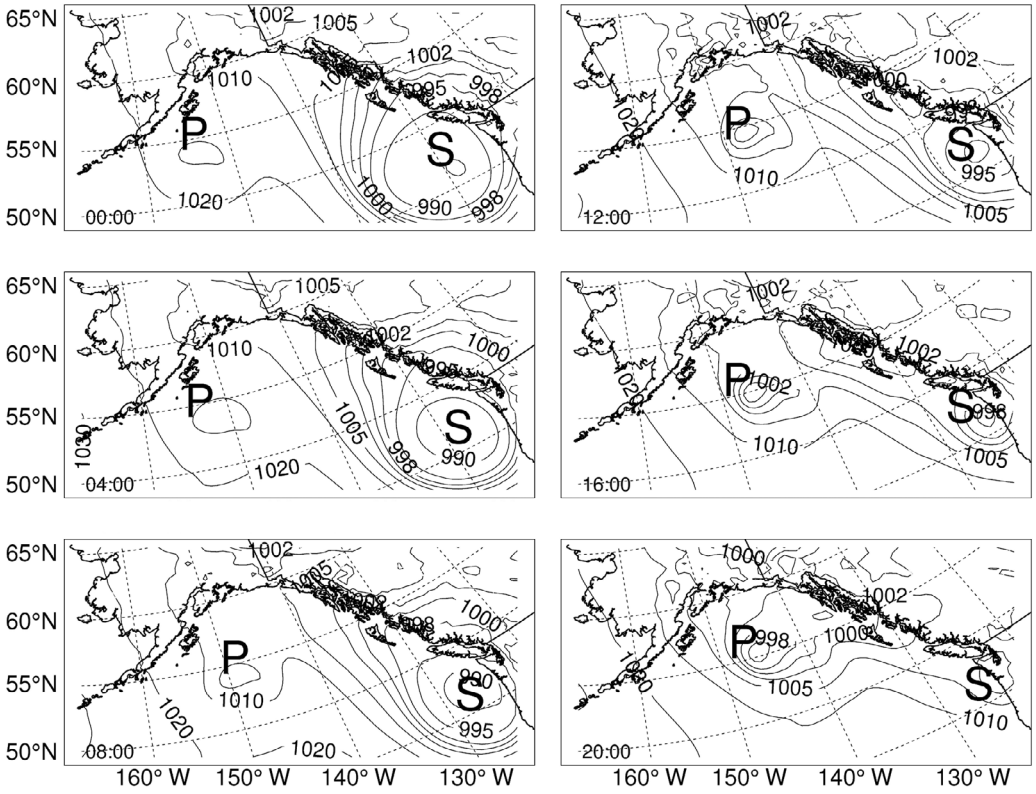

Fig. 6. Mean sea level pressure (SLP) of COSMO-CLM simulation result about the Polar Low on 22th March 1975 in the Gulf of Alaska. P represents the Polar Low and S represents the synoptic low. Left column: maps for 0000, 0400 and 0800 UTC on 22th March 1975; right column: 1200, 1600 and 2000 UTC on 22th March 1975. Figure 6 shows the corresponding satellite image for the bottom left map.

in 6 out of 10 exhibited a deeper minimum pressure value (Table 1). With case 4 there may be a problem in the NCEP reanalysis; the large-scale situation at the lowest level looks rather different, with wind speeds about double of what is described as the wind speed at the 2nd sigma-level (not shown).

We also compared model results with satellite observations, available from detailed studies of the ten cases, and

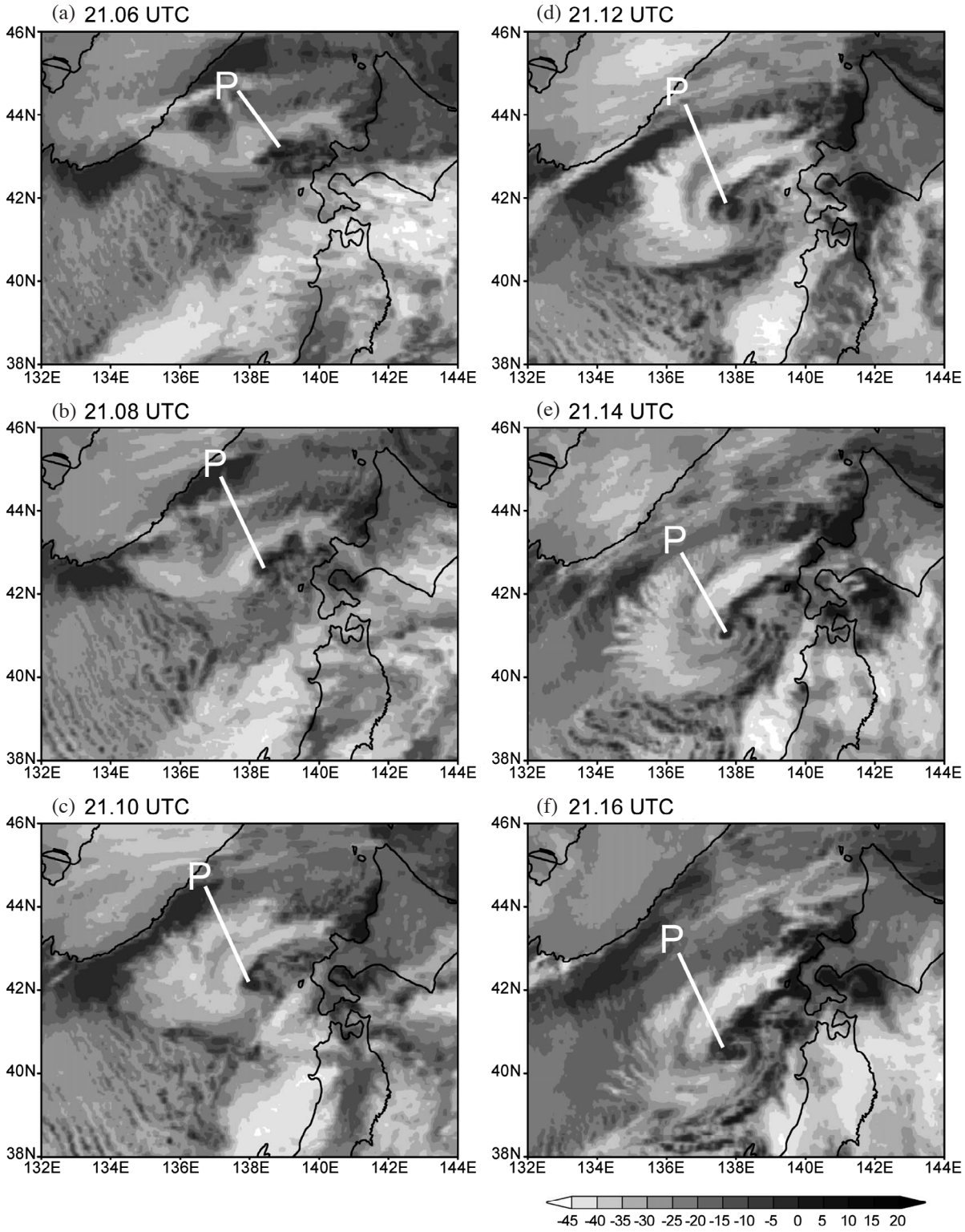

Fig. 7. Two-hourly GMS-5 TBB satellite image from 0600 to 1600 UTC 21th January 1997, Prepresents the Polar Low (Fu et al. 2004a).

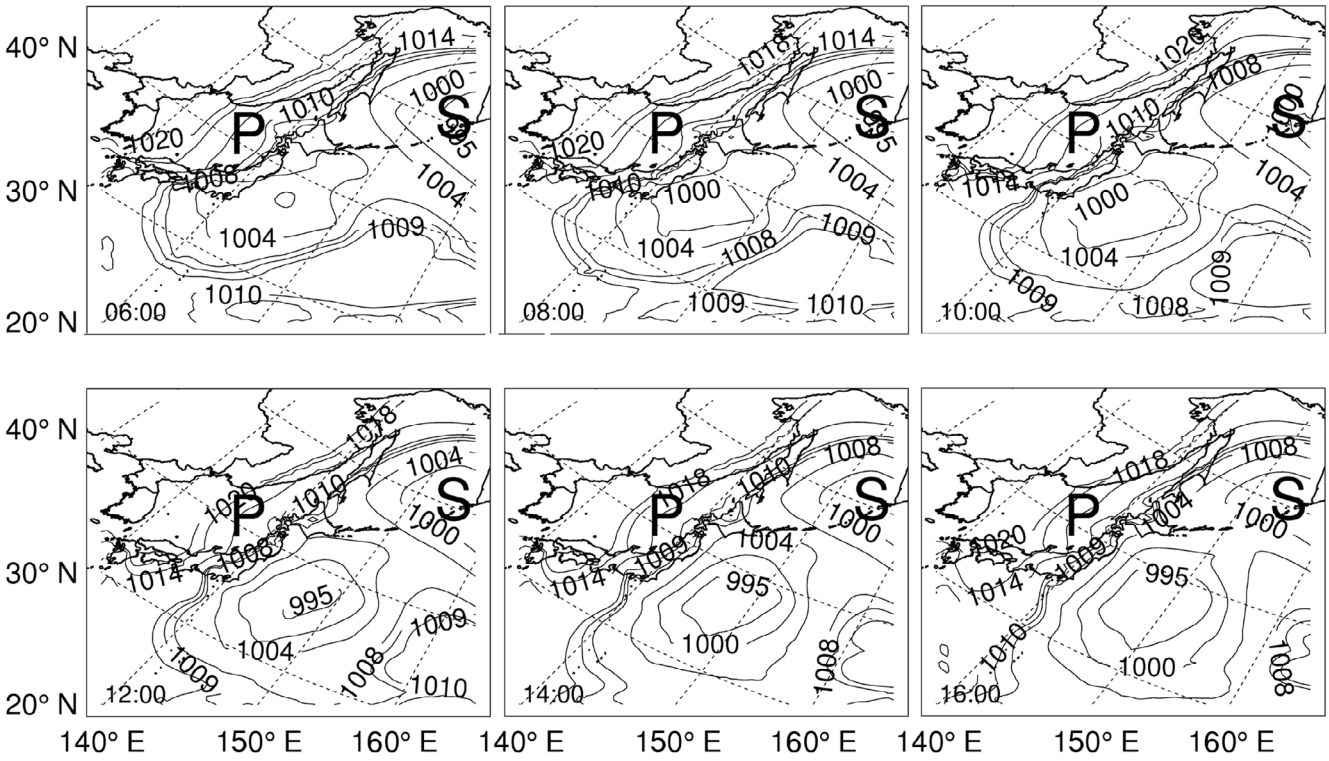

Fig. 8. Mean sea level pressure of COSMO-CLM simulation result about the Polar Low on 21th January 1997 in Japan Sea. P represents the Polar Low and S represents the synoptic low. Top column: maps for 0600, 0800 and 1000 UTC on 21th January 1997; bottom column: 1200, 1400 and 1600 UTC on 21th January 1997.

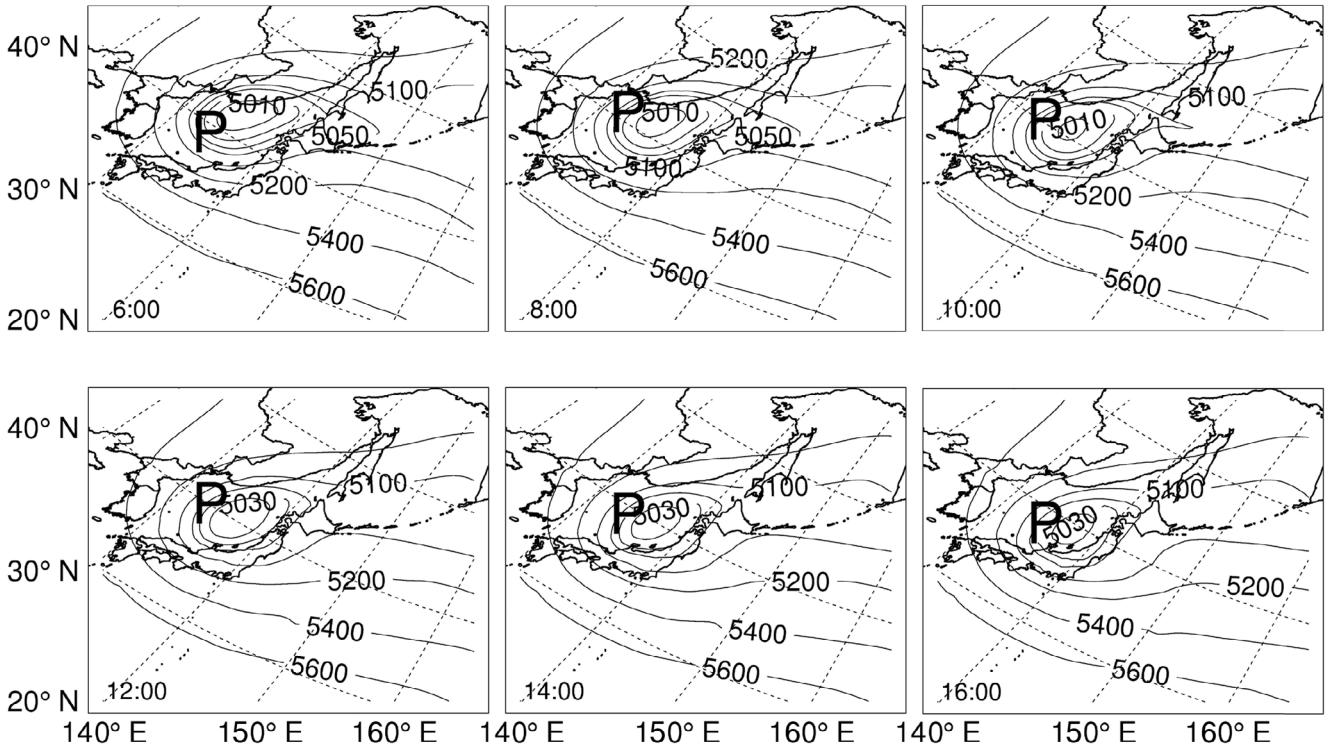

Fig. 9. 500 hPa contour of COSMO-CLM simulation result about the Polar Low on 21th January 1997 in the Japan Sea. P represents the Polar Low. Top column: maps for 0600, 0800 and 1000 UTC on 21th January 1997; bottom column: 1200, 1400 and 1600 UTC on 21th January 1997.

found that our system adds realistic sub-synoptic details consistent with the satellite observations.

We conclude that the model set-up is suitable for simulating Polar Lows statistics (related to the formation and tracks) in the North Pacific. We have recently launched a continuous simulation with CCLM, forced by six decades of NCEP re-analyses. The output of this simulation is searched for the formation and movement of polar lows, and changes from year-to-year as well a trend. In the present study we found that the detection and tracking algorithm needs to be adapted to a somewhat different situation as compared to the North Atlantic. In another paper, we will present these results on North Pacific polar low climatology.

Acknowledgement This work was supported by the Chinese CSC exchange program. The computation was made at German Climate Computing Center DKRZ in Hamburg.

REFERENCES

Blier, W., 1996: A numerical modeling investigation of a case of polar airstream cyclogenesis over the Gulf of Alaska. *Mon. Weather Rev.*, **124**, 2703-2725, doi: 10.1175/1520-0493(1996)124<2703:ANMIOA>2.0.CO;2. [Link]

Bond, N. A. and M. A. Shapiro, 1991: Polar Lows over the Gulf of Alaska in conditions of reverse shear. *Mon. Weather Rev.*, **119**, 551-572, doi: 10.1175/1520-0493(1991)119<0551:PLOTGO>2.0.CO;2. [Link]

Bresch, J. F., R. J. Reed, and M. D. Albright, 1997: A Polar-Low development over the Bering Sea: Analysis, numerical simulation, and sensitivity experiments. *Mon. Weather Rev.*, **125**, 3109-3130, doi: 10.1175/1520-0493(1997)125<3109:APLDOT>2.0.CO;2. [Link]

Businger, S., 1987: The synoptic climatology of polar-low outbreaks over the Gulf of Alaska and the Bering Sea. *Tellus*, **39A**, 307-325, doi: 10.1111/j.1600-0870.1987.tb00310.x. [Link]

Businger, S. and B. Walter, 1988: Comma cloud development and associated rapid cyclogenesis over the Gulf of Alaska: A case study using aircraft and operational data. *Mon. Weather Rev.*, **116**, 1103-1123, doi: 10.1175/1520-0493(1988)116<1103:CCDAAR>2.0.CO;2. [Link]

Carleton, A. M., 1985: Satellite climatological aspects of the "Polar Low" and "instant occlusion". *Tellus*, **37A**, 433-450, doi: 10.1111/j.1600-0870.1985.tb00442.x. [Link]

Cavicchia, L. and H. von Storch, 2012. The simulation of medicanes in a high-resolution regional climate model. *Climate Dyn.*, doi: 10.1007/s00382-011-1220-0, in press. [Link]

Douglas, M. W., L. S. Fedor, and M. A. Shapiro, 1991: Polar Low structure over the northern Gulf of Alaska based on research aircraft observations. *Mon. Weather Rev.*, **119**, 32-54, doi: 10.1175/1520-0493(1991)119<0032:PLSOTN>2.0.CO;2. [Link]

Feser, F., 2006: Enhanced detectability of added value in limited-area model results separated into different spatial scales. *Mon. Weather Rev.*, **134**, 2180-2190, doi: 10.1175/MWR3183.1. [Link]

Feser, F. and H. von Storch, 2005: A spatial two-dimensional discrete filter for limited-area model evaluation purposes. *Mon. Weather Rev.*, **133**, 1774-1786, doi: 10.1175/MWR2939.1. [Link]

Feser, F. and H. von Storch, 2008: Regional modelling of the western Pacific typhoon season 2004. *Meteorol. Z.*, **17**, 519-528, doi: 10.1127/0941-2948/2008/0282. [Link]

Forbes, G. S. and W. D. Lottes, 1985: Classification of mesoscale vortices in polar airstreams and the influence of the large-scale environment on their evolutions. *Tellus*, **37A**, 132-155, doi: 10.1111/j.1600-0870.1985.tb00276.x. [Link]

Fu, G., Q. Liu, and Z. Wu, 1999: General features of polar lows over the Japan Sea and the Northwestern Pacific. *Chin. J. Oceanol. Limnol.*, **17**, 300-307, doi: 10.1007/BF02842823. [Link]

Fu, G., H. Niino, R. Kimura, and T. Kato, 2004a: A Polar Low over the Japan Sea on 21 January 1997. Part I: Observational Analysis. *Mon. Weather Rev.*, **132**, 1537-1551, doi: 10.1175/1520-0493(2004)132<1537:APLOTJ>2.0.CO;2. [Link]

Fu, G., H. Niino, R. Kimura, and T. Kato, 2004b: Multiple polar mesocyclones over the Japan Sea on 11 February 1997. *Mon. Weather Rev.*, **132**: 793-814, doi: 10.1175/1520-0493(2004)132<0793:MPMOTJ>2.0.CO;2. [Link]

Guo, J., G. Fu, Z. Li, L. Shao, Y. Duan, and J. Wang, 2007: Analyses and numerical modeling of a Polar Low over the Japan Sea on 19 December 2003. *Atmos. Res.*, **85**, 395-412, doi: 10.1016/j.atmosres.2007.02.007. [Link]

Kalnay, E., M. Kanamitsu, R. Kistler, W. Collins, D. Deaven, L. Gandin, M. Iredell, S. Saha, G. White, J. Woollen, Y. Zhu, A. Leetmaa, R. Reynolds, M. Chelliah, W. Ebisuzaki, W. Higgins, J. Janowiak, K. C. Mo, C. Ropelewski, and J. Wang, R. Jenne, and D. Joseph, 1996: The NCEP/NCAR 40-year reanalysis project. *Bull. Amer. Meteorol. Soc.*, **77**, 437-471, doi: 10.1175/1520-0477(1996)077<0437:TNYRP>2.0.CO;2. [Link]

Kolstad, E. W., 2006: A new climatology of favourable conditions for reverse-shear Polar Lows. *Tellus*, **58A**, 344-354, doi: 10.1111/j.1600-0870.2006.00171.x. [Link]

Kolstad, E. W., T. J. Bracegirdle, and I. A. Seierstad, 2009: Marine cold-air outbreaks in the North Atlantic: Temporal distribution and associations with large-scale atmospheric circulation. *Climate Dyn.*, **33**, 187-197, doi: 10.1007/s00382-008-0431-5. [Link]

Mailhot, J., D. Hanley, B. Bilodeau, and O. Hertzman, 1996:

A numerical case study of a polar low in the Labrador Sea. *Tellus*, **48A**, 383-402, doi: 10.1034/j.1600-0870.1996.t01-2-00003.x. [Link]

Nordeng, T. E., 1990: A model-based diagnostic study of the development and maintenance mechanism of two polar lows. *Tellus*, **42A**, 92-108, doi: 10.1034/j.1600-0870.1990.00009.x. [Link]

Rockel, B., A. Will, and A. Hense, 2008: The regional climate model COSMO-CLM (CCLM). *Meteorol. Z.*, **17**, 347-348, doi: 10.1127/0941-2948/2008/0309. [Link]

Steppeler, J., G. Doms, U. Schättler, H. W. Bitzer, A. Gassmann, U. Damrath, and G. Gregoric, 2003: Meso-gamma scale forecasts using the nonhydrostatic model LM. *Meteorol. Atmos. Phys.*, **82**, 75-96, doi: 10.1007/s00703-001-0592-9. [Link]

von Storch, H., H. Langenberg, and F. Feser, 2000: A spectral nudging technique for dynamical downscaling purposes. *Mon. Weather Rev.*, **128**, 3664-3673, doi: 10.1175/1520-0493(2000)128<3664:ASNTFD>2.0.CO;2. [Link]

Weisse, R. and F. Feser, 2003: Evaluation of a method to reduce uncertainty in wind hindcasts performed with regional atmosphere models. *Coast. Eng.*, **48**, 211-225, doi: 10.1016/S0378-3839(03)00027-9. [Link]

Wu, L. and G. W. Petty, 2010: Intercomparison of bulk microphysics schemes in model simulations of polar lows. *Mon. Weather Rev.*, **138**, 2211-2228, doi: 10.1175/2010MWR3122.1. [Link]

Yanase, W. and H. Niino, 2007: Dependence of Polar Low development on baroclinicity and physical processes: An idealized high-resolution numerical experiment. *J. Atmos. Sci.*, **64**, 3044-3067, doi: 10.1175/JAS4001.1. [Link]

Yanase, W., G. Fu, H. Niino, and T. Kato, 2004: A Polar Low over the Japan Sea on 21 January 1997. Part II: A numerical study. *Mon. Weather Rev.*, **132**, 1552-1574, doi: 10.1175/1520-0493(2004)132<1552:APLOTJ>2.0.CO;2. [Link]

Yarnal, B. and K. G. Henderson, 1989a: A climatology of Polar Low cyclogenetic regions over the North Pacific Ocean. *J. Climate*, **2**, 1476-1491, doi: 10.1175/1520-0442(1989)002<1476:ACOPLC>2.0.CO;2. [Link]

Yarnal, B. and K. G. Henderson, 1989b: A satellite-derived climatology of polar-low evolution in the North Pacific. *Int. J. Climatol.*, **9**, 551-566, doi: 10.1002/joc.3370090602. [Link]

Zahn, M. and H. von Storch, 2008a: Tracking Polar Lows in CLM. *Meteorol. Z.*, **17**, 445-453, doi: 10.1127/0941-2948/2008/0317. [Link]

Zahn, M. and H. von Storch, 2008b: A long-term climatology of North Atlantic polar lows. *Geophys. Res. Lett.*, **35**, L22702, doi: 10.1029/2008GL035769. [Link]

Zahn, M., H. von Storch, and S. Bakan, 2008: Climate mode simulation of North Atlantic Polar Lows in a limited area model. *Tellus*, **60A**, 620-631, doi: 10.1111/j.1600-0870.2008.00330.x. [Link]